

# Algorithm to Calculate the Partition Function for Z(2) Lattice Gauge Theory in Four Dimensions

HIROAKI ARISUE

*Osaka Prefectural College of Technology, Neyagawa, Osaka 572, Japan*

TOSHIAKI FUJIWARA

*College of Liberal Arts and Sciences, Kitasato University, Sagamihara, Kanagawa 228, Japan*

AND

YUMI S. HIRATA

*Kyoai gakuen Women's Junior College, Maebashi, Gunma 379-21, Japan*

Received May 6, 1991; revised August 30, 1993

---

An algorithm is shown for the calculation of the exact partition function of finite system in four-dimensional Z(2) lattice gauge theory. The partition functions to the size  $2 \times 2 \times 2 \times 1$  are given. From them, zero-point distribution of the partition functions and the strong coupling expansion of the free energy to the order of  $u^{24}$  are shown.

© 1994 Academic Press, Inc.

---

## I. INTRODUCTION

The analytical calculation of the partition function of lattice gauge theory in finite size systems gives much information about the structure of the theory. For example, the zero-point distribution of the partition function in the complex coupling-constant plane gives information about the phase transition in the theory [1, 2]. The section of the distribution to the real axis shows the location of phase transition points and the order of the transition. In another example, analytical calculation of the partition functions of size  $X + Y + Z + T \leq L$  for given  $L$  ( $X, Y, Z, T$  is the space/time length of the finite system) leads the strong coupling expansion of the free energy to  $u^{4(L-1)}$  using the new cluster expansion [3]. For the extrapolation of the approximations to infinite size, calculations for large systems are indispensable.

Calculation of the partition function for Z(2) lattice gauge theory is equivalent to counting all closed surfaces in the lattice space-time  $V_4 = X \times Y \times Z \times T$ . There are  $2^{(3XYZT + XYZ + XYT + XZT + YZT)}$  closed surfaces in  $V_4$ . Efficient algorithms are desired for counting the closed surfaces. In this paper, we show an algorithm that costs

$T(2XYZ + XY + YZ + ZX) 2^{(2XYZ + XY + YZ + ZX)}$  steps. Using this algorithm we have calculated the exact partition function for systems with  $X + Y + Z + T \leq 7$ .

In Section II, we describe the algorithm; in Section III, zero-point distribution of the partition functions is shown; in Section IV, the strong expansion for the four-dimensional Z(2) lattice gauge theory to  $u^{24}$  is given. Section V is devoted to conclusion and discussion.

## II. FORMULATION

The partition function of the four-dimensional isotropic Z(2) lattice gauge theory with standard action [4] is

$$Z \equiv \sum_{\{\sigma_l\}} \exp \left( \sum_p \beta \sigma_p \right) = \left( \prod_p \cosh \beta \right) Z^*, \quad (2.1)$$

where

$$Z^* = \sum_{\{\sigma_l\}} \prod_p (1 + u \sigma_p). \quad (2.2)$$

Here,  $\sigma_p$  in Eq. (2.1) is the product of four link variables  $\sigma_l$  around a plaquette  $p$ ,

$$\sigma_p = \prod_{l \in \partial p} \sigma_l. \quad (2.3)$$

$\beta$  is a coupling constant, and  $u = \tanh \beta$ . The summation in Eqs. (2.1)–(2.2) is the average for link variables  $\sigma_l$ ,

$$\sum_{\{\sigma_l\}} \cdot \equiv \frac{1}{2} \sum_{\sigma_1 = \pm 1} \frac{1}{2} \sum_{\sigma_2 = \pm 1} \cdots \cdot \quad (2.4)$$

Equation (2.1) works on a four-dimensional Euclidean lattice of size  $V_4 = V_3 \times T$  with free boundary condition.

$Z^*$  in Eq. (2.2) can be rewritten as

$$Z^* = \text{singlet part of } \left\{ \prod_{p \in V_4} (1 + u\sigma_p) \right\}, \quad (2.5)$$

$$= \sum_{\text{all closed surfaces } S \text{ in } V_4} u^{\|S\|}, \quad (2.6)$$

where  $\|S\|$  is the number of plaquettes which form closed surface  $S$ . A closed surface is a set of plaquettes and every link is shared by even number of the plaquettes. Because  $\sigma_l^{\text{odd}} = \sigma_l$  ( $= Z(2)$  doublet),  $\sigma_l^{\text{even}} = 1$  ( $= Z(2)$  singlet) and  $\frac{1}{2} \sum_{\sigma_l = \pm 1} \sigma_l = 0$ ,  $\frac{1}{2} \sum_{\sigma_l = \pm 1} 1 = 1$ , for arbitrary link  $l$ .

*First step.* Definitions of potential and kinetic terms. We decompose these plaquettes in  $V_4$  to a direct sum of sets of plaquettes  $\mathbf{P}(0)$  (set of space-like plaquettes at  $t=0$ ),  $\mathbf{P}(1)$ ,  $\mathbf{P}(2)$ , ...,  $\mathbf{P}(T)$ , and  $\mathbf{P}(0, 1)$  (the set of time-like plaquettes between  $t=0$  and  $t=1$ ),  $\mathbf{P}(1, 2)$ ,  $\mathbf{P}(2, 3)$ , ...,  $\mathbf{P}(T-1, T)$ . We define  $\Phi$  and  $K$  as

$$\Phi(t) \equiv \prod_{p \in \mathbf{P}(t)} (1 + u\sigma_p), \quad (2.7)$$

$$K(t, t+1) \equiv \prod_{p \in \mathbf{P}(t, t+1)} (1 + u\sigma_p). \quad (2.8)$$

We call  $\Phi(t)$  a potential term and  $K(t, t+1)$  a kinetic term.

Then  $Z^*$  in Eq. (2.5) is rewritten as

$$Z^* = \text{singlet part of } \left\{ \left[ \prod_{0 \leq t \leq T-1} \Phi(t) K(t, t+1) \right] \Phi(T) \right\}. \quad (2.9)$$

*Second step.* Introduction of loop representations. Integrate all of the time-like link variables in Eq. (2.8). Consider an arbitrary time-like link  $l$ . If odd number of plaquettes share this link  $l$ , this term will vanish after the integration. Then non-vanishing terms after the integration consist of contributions from closed loops as shown in Fig. 1. A closed loop  $L_i$  is a set of links and every site is shared by even number of the links. Let  $L$  be set of closed loops drawn in  $V_3$ . Thus we obtain

$$K(t, t+1) = \sum_{\{L_i \in L\}} \sigma^{(t)}(L_i) \sigma^{(t+1)}(L_i) u^{\|L_i\|} + O, \quad (2.10)$$

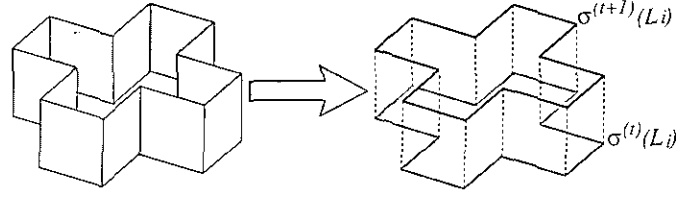


**FIG. 1.** Integration of time-like links yields identical twins of closed loops at time  $t$  and  $t+1$ . (Left) Before integration. A diagram made of 12 plaquettes is shown. (Right) After the integration. Black (at  $t+1$ ) and gray (at  $t$ ) loop at the identical twins whose length is 12.

where  $\|L_i\|$  is the length of  $L_i$ . Suffix  $t$  or  $t+1$  is marked for making it clear that the loop variable exists at  $t$  or  $t+1$ . The loop variable  $\sigma^{(t)}(L_i)$  is the product of the space-like link variable along  $L_i$ ,

$$\sigma(L_i) = \prod_{l \in L_i} \sigma_l. \quad (2.11)$$

The last term  $O$  in Eq. (2.10) represents terms which will vanish after the integration of the time-like link variables.

Now consider the function  $\Phi(t)$ ; the product of an arbitrary set of plaquette variables makes a closed loop. But many different sets of plaquettes can make the same closed loop. So, we first add the contributions from every set of plaquettes whose boundary is a closed loop  $L_i$ ; then we add the contributions from the  $L_i$ 's. That is,

$$\Phi(t) = \sum_{L_i} \sigma^{(t)}(L_i) \varphi(i), \quad (2.12)$$

$$\varphi(i) \equiv \sum_{\{S \text{ such that } \partial S = L_i\}} u^{\|S\|}, \quad (2.13)$$

where  $S$  is the set of plaquettes in  $V_3$  and  $\|S\|$  is the number of the plaquettes in  $S$ .

In Appendix A, it is shown that there is a one-to-one correspondence between a closed loop and an integer (thus we write  $\sigma(L_i)$  as  $\sigma(i)$ ) which has the following property:

$$\sigma(i) \cdot \sigma(j) = \sigma(i * j), \quad (2.14)$$

$$\sigma(i) = 1, \quad \text{if and only if } i = 0. \quad (2.15)$$

Star product ( $*$ ) in the Eq. (2.14) represents the “exclusive OR” in the bit-operation of integers.

*Third step.* Loop representation of the partition function. Consider the fate of a closed loop at a time  $t$  after the integrations of space-like link variables. Variable  $\sigma^{(t)}$  appears in three places,  $K(t-1, t)$ ,  $\Phi(t)$ , and  $K(t, t+1)$ . Let us consider a given loop  $i$  in  $K(t-1, t)$ , a given loop  $j$  in

$K(t, t+1)$ , and all the loops in  $\Phi(t)$ . This part of Eq. (2.9) looks like

$$\begin{aligned} & \underbrace{\cdots \sigma^{(t)}(i)}_{K(t-1,t)} \underbrace{\left( \sum_k \sigma^{(t)}(k) \varphi(i) \right)}_{\Phi(t)} \underbrace{\sigma^{(t)}(j) \cdots}_{K(t,t+1)} \\ & = \cdots \sum_k \varphi(i) \sigma^{(t)}(i * j * k) \cdots \end{aligned} \quad (2.16)$$

After integrations of the space-like link variables at time  $=t$ , only singlet term  $i * j * k = 0$ , i.e.,  $k = i * j$ , will survive. Thus Eq. (2.16) becomes equal to

$$\cdots \varphi(i * j) \cdots + O, \quad (2.17)$$

where the last term  $O$  represents terms which will vanish after the integration of the space-like link variables. Thus the partition function  $Z^*$  is written as

$$\begin{aligned} Z^* &= \sum_{i_1, i_2, \dots, i_T} \varphi^{(i_1)} u^{\|L(i_1)\|} \varphi(i_1 * i_2) u^{\|L(i_2)\|} \\ & \cdots \varphi(i_{T-1} * i_T) u^{\|L(i_T)\|} \varphi(i_T). \end{aligned} \quad (2.18)$$

Methods to calculate  $\|L(i)\|$  and  $\varphi(i)$  are shown in Appendices B and C.

Let us introduce matrix representation for  $\varphi$ ,  $K$ ,

$$\varphi_{i,j} \equiv \varphi(i * j), \quad (2.19)$$

$$K_{i,j} \equiv u^{\|L(i)\|} \delta_{i,j}; \quad (2.20)$$

then we obtain

$$Z^* = (\varphi K \varphi K \cdots \varphi)_{0,0}. \quad (2.21)$$

*The final step.* Diagonalize the potential term. There are  $2^{(N_p - V_3)}$  closed loops in  $V_3$ , where  $N_p = 3XYZ + XY + YZ + ZX$  is the number of plaquettes in  $V_3$  and  $V_3 = XYZ$  is the volume. Therefore the  $i$ 's in Eq. (2.18) run from zero to  $2^{(N_p - V_3)} - 1$ . Then  $T \times 4^{(N_p - V_3)}$  steps would be needed to calculate the partition function in the equation (2.18) or (2.21). This is because the potential term is not diagonal for closed loop representation. To diagonalize the matrix  $\varphi$ , we introduce a fourier transform as

$$F_{i,j} \equiv (-1)^{\|i * j\|}, \quad (2.22)$$

where dot product ( $\cdot$ ) represents "AND" in bit-operation of integers, and double fence ( $\|\cdots\|$ ) is "bit-counter" that counts the number of non-zero bits,

$$\|a\| \equiv \sum_n a_n \quad \text{for} \quad a = \sum_n a_n 2^n \quad (a_n = 0 \text{ or } 1). \quad (2.23)$$

Note that the fourier matrix is order 2 (own inversion),

$$\frac{1}{N} FF = \mathbf{1}, \quad (2.24)$$

where normalization factor  $N = 2^{(N_p - V_3)}$  is the number of the closed loops. As shown in Appendix D, the fourier transformed potential  $\tilde{\varphi}$  is diagonal,

$$\begin{aligned} \tilde{\varphi}_{i,j} &\equiv (F\varphi F^{-1})_{i,j} \\ &= \tilde{\varphi}_i \delta_{i,j}, \end{aligned} \quad (2.25)$$

where

$$\begin{aligned} \tilde{\varphi}_i &\equiv (F\varphi)_i \\ &= \sum_k (-1)^{\|i * k\|} \varphi(k). \end{aligned} \quad (2.26)$$

Thus we obtain the final expression for the partition function  $Z^*$ ,

$$\begin{aligned} Z^* &= (\varphi KF^{-1} \tilde{\varphi} FKF^{-1} \tilde{\varphi} FKF^{-1} \cdots F^{-1} \tilde{\varphi} FKF)_{0,0} \\ &= \frac{1}{N^{(T-1)}} (\varphi KF \tilde{\varphi} FKF \tilde{\varphi} FKF \cdots F \tilde{\varphi} FKF)_{0,0}. \end{aligned} \quad (2.27)$$

In the above, non-diagonal matrices  $\varphi$  at far-left and far-right in the parenthesis is harmless because their left or right index is fixed to zero. The only remaining non-diagonal

TABLE I  
Finite Systems We Have Calculated

$L$	$T$	$X$	$Y$	$Z$
3	0	1	1	1
4	0	2	1	1
	1	1	1	1
5	0	3	1	1
	0	2	2	1
	2	1	1	1
6	0	2	2	2
	0	3	2	1
	0	4	1	1
	1	3	1	1
	2	2	1	1
7	0	5	1	1
	0	4	2	1
	0	3	3	1
	0	3	2	2
	1	4	1	1
	2	3	1	1
	2	2	2	1

TABLE II

Coefficients of the Partition Function of  $V_4 = 2 \times 2 \times 2 \times 1$ ,  
where  $Z^* = \sum_i a_i u^i$

$i$	$a_i$	$i$	$a_i$	$i$	$a_i$
0	1	40	3658414290	80	11920348335
2	0	42	8903009272	82	2687300304
4	0	44	20811640692	84	493591960
6	52	46	46508648040	86	72601968
8	0	48	98842022652	88	8294196
10	252	50	198489897816	90	721736
12	1394	52	373906469136	92	41004
14	1548	54	655166465536	94	1128
16	12045	56	1057602913950	96	10
18	35064	58	1555921141776		
20	95592	60	2062894008816		
22	358608	62	2437561122960		
24	1015206	64	2538774701679		
26	3107592	66	2305843274872		
28	9330468	68	1807554017112		
30	26517896	70	1211287012500		
32	75467982	72	687883487670		
34	207554664	74	328512456876		
36	556546328	76	131083824474		
38	1450827768	78	43467741196		

matrix is the fourier matrix  $F$ . Fortunately, it needs only  $(N_p - V_3) 2^{(N_p - V_3)}$  steps, instead of  $4^{(N_p - V_3)}$  steps, to perform fourier transformation by virtue of the fast Fourier transform algorithm. This will be discussed in Appendix D. Thus  $T(N_p - V_3) 2^{(N_p - V_3)}$  steps are needed to calculate the partition function.

Before closing this section, we write here the explicit form of the partition function for  $T = 1$  and  $T = 2$ ,

$$Z^* = \begin{cases} (\varphi K \varphi)_{0,0} & \text{for } T = 1, \\ \frac{1}{N} (\varphi K F \tilde{\varphi} F K \varphi)_{0,0} & \text{for } T = 2. \end{cases} \quad (2.28)$$

Using this algorithm, we have calculated exact partition function for systems with  $X + Y + Z + T \leq 7$  (see Table I). Exact partition function of  $2 \times 2 \times 2 \times 1$  is shown in Table II. CPU time for calculating the partition function was several tens minute using FACOM M780.

### III. ZERO-POINT DISTRIBUTION OF $Z^*$

From self-duality and data of Monte-Carlo simulations, [5] it has been confirmed that the first-order phase transition occur at the self-dual point,  $\beta_{\text{selfdual}} = \ln(1 + \sqrt{2}) \cong 0.4407$ ,  $u_{\text{selfdual}} = \sqrt{2} - 1 \cong 0.4142$ . Zero-point distribution of the partition function in  $\beta$ ,  $\beta^*$ ,  $u$ , and  $u^*$  are shown in Fig. 2. The suffix \* denotes dual. For the finite systems with the free boundary condition that we have used, self-duality

is not exact. The distributions in  $2 \times 2 \times 2 \times 1$  are inclined so that the section for the real axis is  $\beta_c = 0.6$  and  $\beta_c^* = 0.3$ .  $\beta_c$  and  $\beta_c^*$  are far from the self-dual point  $\beta_{\text{selfdual}}$  and  $\beta_c \neq \beta_c^*$ . It is expected that in a larger system  $\beta_c$  and  $\beta_c^*$  come near  $\beta_{\text{selfdual}}$ . Furthermore, global distributions are interesting in studying of the analytical feature of  $Z$ . Partition functions in larger systems are requested.

### IV. NEW CLUSTER EXPANSION AND STRONG COUPLING EXPANSION FOR THE FREE ENERGY

Using the partition functions of the finite systems with  $X + Y + Z + T \leq 7$  we find the new cluster expansion [3] of thermodynamical functions. This expansion is one of the cluster expansions whose expansion parameter is in space-time. As the zeroth-order approximation, the leading term in the conventional strong coupling expansion is taken. The  $L$ th-order term contains all the effects of the correlation among the plaquette variables at the  $L$  lattice spacing. In Fig. 3 the new cluster expansion of the internal energy to  $L = 7$  is shown [6]. The jump in the internal energy at  $\beta_{\text{selfdual}}$  is shown in Fig. 3.

Performing Taylor expansion of the thermodynamical function with respect to  $\beta$  (or  $u$ ) in the midst of the algorithm of the new cluster expansion leads the strong coupling series of the thermodynamical function to  $4L - 4$ . We obtain the strong coupling expansion of the free energy to  $u^{24}$ ,

$$\begin{aligned} f &\equiv \lim_{V_4 \rightarrow \infty} \frac{1}{V_4} \log Z \\ &= 6 \log \cosh \beta \\ &\quad + 4u^6 + 36u^{10} + 2u^{12} + 468u^{14} - 81u^{16} \\ &\quad + 7377 \frac{1}{3} u^{18} - 2070u^{20} + 132,204u^{22} \\ &\quad - 45,781u^{24} + O(u^{26}), \end{aligned} \quad (4.1)$$

where coefficients to  $u^{22}$  coincide with Wilson's results [7]. (The coefficient of  $u^{24}$  term is newly obtained.)

### V. CONCLUSION AND DISCUSSION

In this paper an algorithm for the calculation of the partition function of  $Z(2)$  lattice gauge theory in four dimensions has been shown. Using this algorithm, the partition functions for the system with  $X + Y + Z + T \leq 7$  has been computed. Zero-point distribution of the partition function has been shown. Furthermore, the cluster expansion of some thermodynamical functions have been calculated. Especially the strong coupling expansion of the free energy to  $u^{24}$  has been estimated.

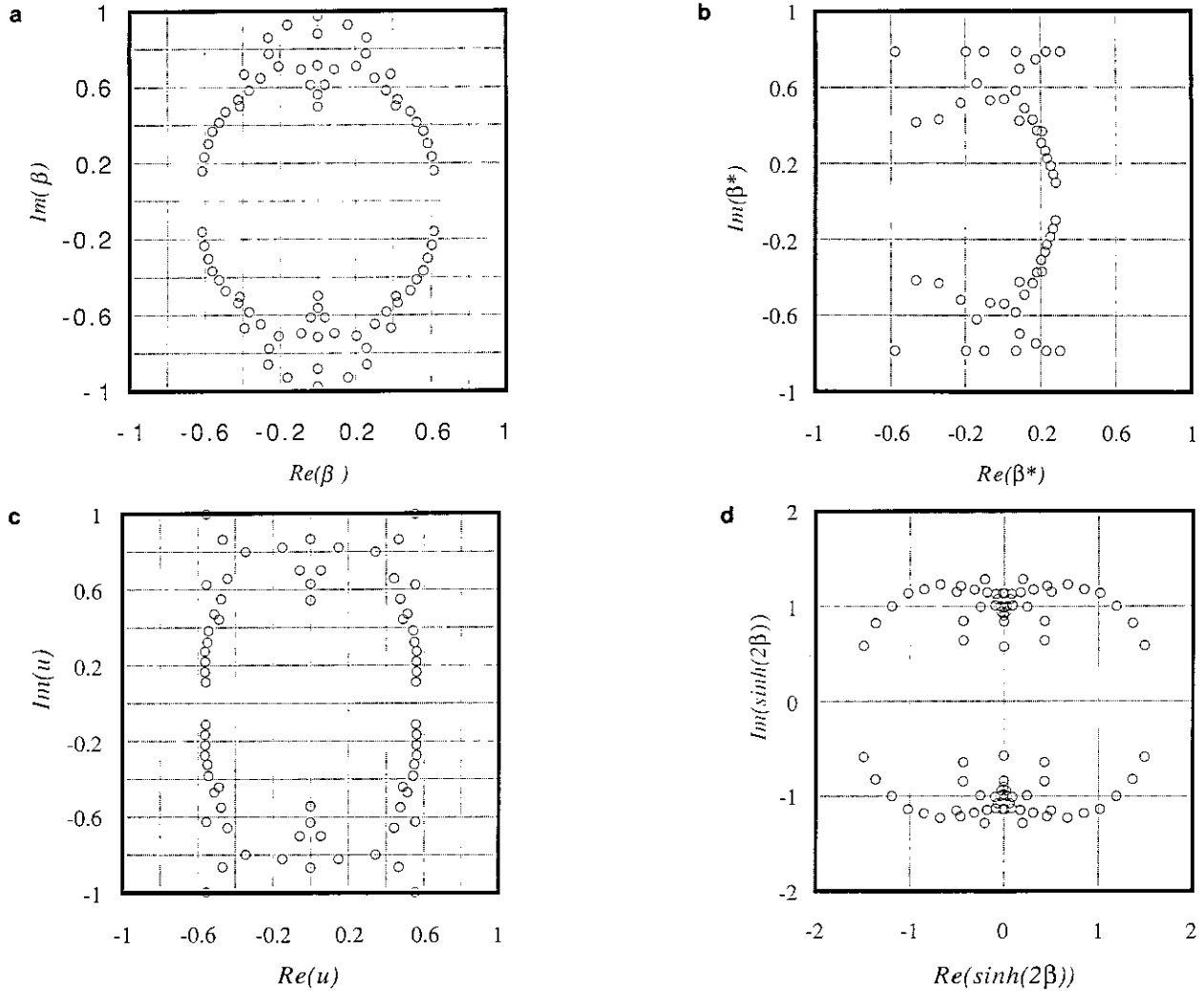


FIG. 2. Distribution of zero-point of partition function of  $V_4 = 2 \times 2 \times 2 \times 1$  in (a) coupling constant  $\beta$ -plane, (b) dual coupling constant  $\beta^*$ -plane, (c)  $u = \tanh(\beta)$  plane, and (d)  $\sinh(2\beta)$  plane.

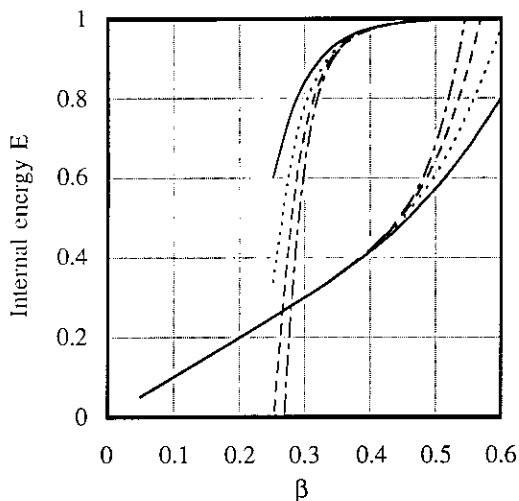


FIG. 3. The new cluster expansion of internal energy  $E \equiv 1/6 (df/d\beta)$  is plotted as a function of  $\beta$ . The solid line, dotted line, dashed line, and dot-dashed line denote the energy for  $L = 4, 5, 6,$  and  $7$ , respectively.

Important points of our algorithm are

- (1) we have introduced closed-loop representation that is expressed by integers,
- (2) the product of two closed  $Z(2)$ -loops is expressed by the “exclusive OR” of integers that represent these loops,
- (3) the non-diagonal potential term is diagonalized by the Fourier transformation,
- (4) the fast fourier algorithm is used.

Our method, however, needs large memory space to store the state vectors,  $(\varphi)_{i,0}$  or  $(K\varphi)_{i,0}$  or  $(FK\varphi)_{i,0}$  or  $\dots$ , in Eq. (2.27). For example, calculation of the partition function for  $V_4 = 2 \times 2 \times 2 \times 1$  needs 11 Mb. This is the weak point of this algorithm. This point must be overcome to calculate the partition function for larger systems.

### APPENDIX A: CLOSED LOOPS IN THREE-DIMENSIONAL LATTICE SYSTEM

Let  $\mathbf{P}$  be a set of the plaquettes in  $V_3$ ,

$$\mathbf{P} \equiv \{p_0, p_1, \dots, p_k, \dots, p_{N_p-1}\}. \quad (\text{A.1})$$

Let  $P$  be a subset of  $\mathbf{P}$ . There exist  $2^{N_p}$  subsets. A subset  $P$  defines an integer as

$$i \equiv \sum_{0 \leq k \leq N_p-1} a_k 2^k, \quad (\text{A.2})$$

where

$$a_k = \begin{cases} 0 & \text{for } p_k \notin P, \\ 1 & \text{for } p_k \in P. \end{cases} \quad (\text{A.3})$$

On the other hand, integer  $i$  defines a subset  $P_i$  and a closed loop  $\sigma(i)$ :

$$\sigma(i) \begin{cases} \equiv \prod_{p \in P_i} \sigma_p & \text{for } P_i \neq \text{null set}, \\ \equiv 1 & \text{for } P_i = \text{null set}. \end{cases} \quad (\text{A.4})$$

Consider the product of two closed loops  $\sigma(i)$  and  $\sigma(j)$ . Because of  $(\sigma_p)^2 = 1$  we obtain

$$\begin{aligned} \sigma(i) \sigma(j) &= \left( \prod_{p \in P_i} \sigma_p \right) \left( \prod_{p \in P_j} \sigma_p \right) \\ &= \prod_{p \in (P_i \cup P_j - P_i \cap P_j)} \sigma_p. \end{aligned} \quad (\text{A.5})$$

In the above, the set in the second line is the set defined by the integer  $i * j$  (exclusive OR of  $i$  and  $j$ ),

$$P_i \cup P_j - P_i \cap P_j = P_{i * j}. \quad (\text{A.6})$$

Thus we obtain a rule for loop product,

$$\sigma(i) \sigma(j) = \sigma(i * j). \quad (\text{A.7})$$

A closed surface is the special case of closed loop, i.e., a vanishing loop,

$$\sigma(m) = 1. \quad (\text{A.8})$$

We know that the number of closed surfaces is  $2^{V_3}$ . Therefore we number the solutions of Eq. (A.8) as

$$\sigma(m_i) = 1, \quad 0 \leq i \leq 2^{V_3} - 1. \quad (\text{A.9})$$

**THEOREM 1.** For any closed loop  $\sigma(i)$ ,  $2^{V_3}$  plaquette configurations describe the same closed loop. Thus the number of the closed loops is  $2^{(N_p - V_3)}$ .

*Proof.* Let  $j = i * m_k$ , where  $m_k$  is a solution in Eq. (A.9). Then  $j$  represents the same closed loop as  $i$ ; therefore  $\sigma(j) = \sigma(i * m_k) = \sigma(i) \sigma(m_k) = \sigma(i)$ . The reverse is the following. If  $\sigma(i) = \sigma(j)$ , then  $1 = \sigma(i) \sigma(j) = \sigma(i * j)$ . Therefore  $i * j$  is a solution of Eq. (A.9) and  $\exists$  an  $m_k$  such that  $m_k = i * j$ . Thus  $j = i * m_k$ . Q.E.D.

To achieve one-to-one correspondence between a closed loop and an integer, we restrict the set of plaquette,

$$\tilde{\mathbf{P}} \equiv \{p_0, p_1, \dots, p_{N_p - V_3 - 1}\}. \quad (\text{A.10})$$

$\tilde{\mathbf{P}}$  is chosen so that any subset of  $\tilde{\mathbf{P}}$  does not represent a closed surface except for the null set. An example of  $\tilde{\mathbf{P}}$  are "key boxes" shown in Fig. 4. In the "key boxes" shown in Fig. 4, all the plaquettes on the  $z = \text{const}$  planes, except for  $z = 0$ , are removed. The set  $\tilde{\mathbf{P}}$  inherits the properties of (A.2)–(A.7). Equation (A.8) is satisfied only by  $m = 0$ , by the definition

$$\sigma(m) \begin{cases} = 1 & \text{for } m = 0, \\ \neq 1 & \text{for } 1 \leq m \leq 2^{(N_p - V_3)} - 1. \end{cases} \quad (\text{A.11})$$

**THEOREM 2.** In  $\tilde{\mathbf{P}}$ , closed loops correspond one-to-one to plaquette configurations.

*Proof.* The number of the subset of  $\tilde{\mathbf{P}}$  is the same as the number of closed loops  $2^{(N_p - V_3)}$ . And if  $i \neq j$  ( $0 \leq i, j \leq 2^{N_p - V_3} - 1$ ), then  $0 < i * j \leq 2^{N_p - V_3} - 1$ . Thus by the above equation,  $\sigma(i) \sigma(j) = \sigma(i * j) \neq 1$ ; therefore  $\sigma(i) \neq \sigma(j)$ . Q.E.D.

### APPENDIX B: CALCULATIONS OF $\|L_i\|$

We chose the system of "key boxes" shown in Fig. 4 as  $\tilde{\mathbf{P}}$ . We assign Z-bit integers  $\xi_{x,y}$  ( $0 \leq x \leq X, 1 \leq y \leq Y$ ) for plaquettes on  $x = \text{const}$  planes,  $\eta_{x,y}$  ( $1 \leq x \leq X, 0 \leq y \leq Y$ ) for those on  $y = \text{const}$  planes and 1-bit integers  $\zeta_{x,y}$  ( $1 \leq x \leq X, 1 \leq y \leq Y$ ) for those on  $z = 0$ . See Fig. 5. Closed

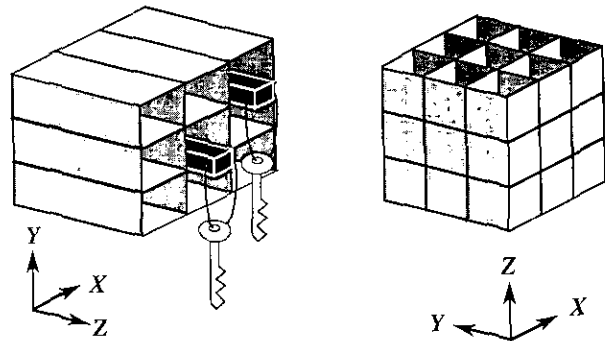


**FIG. 4.** Key boxes in hotel counter is an example of the set  $\tilde{\mathbf{P}}$ . (Left) Key boxes and keys as ordinary view. (Right) Key boxes made of plaquettes. We have removed plaquettes on  $z = \text{constant}$  plane except for  $z = 0$ .

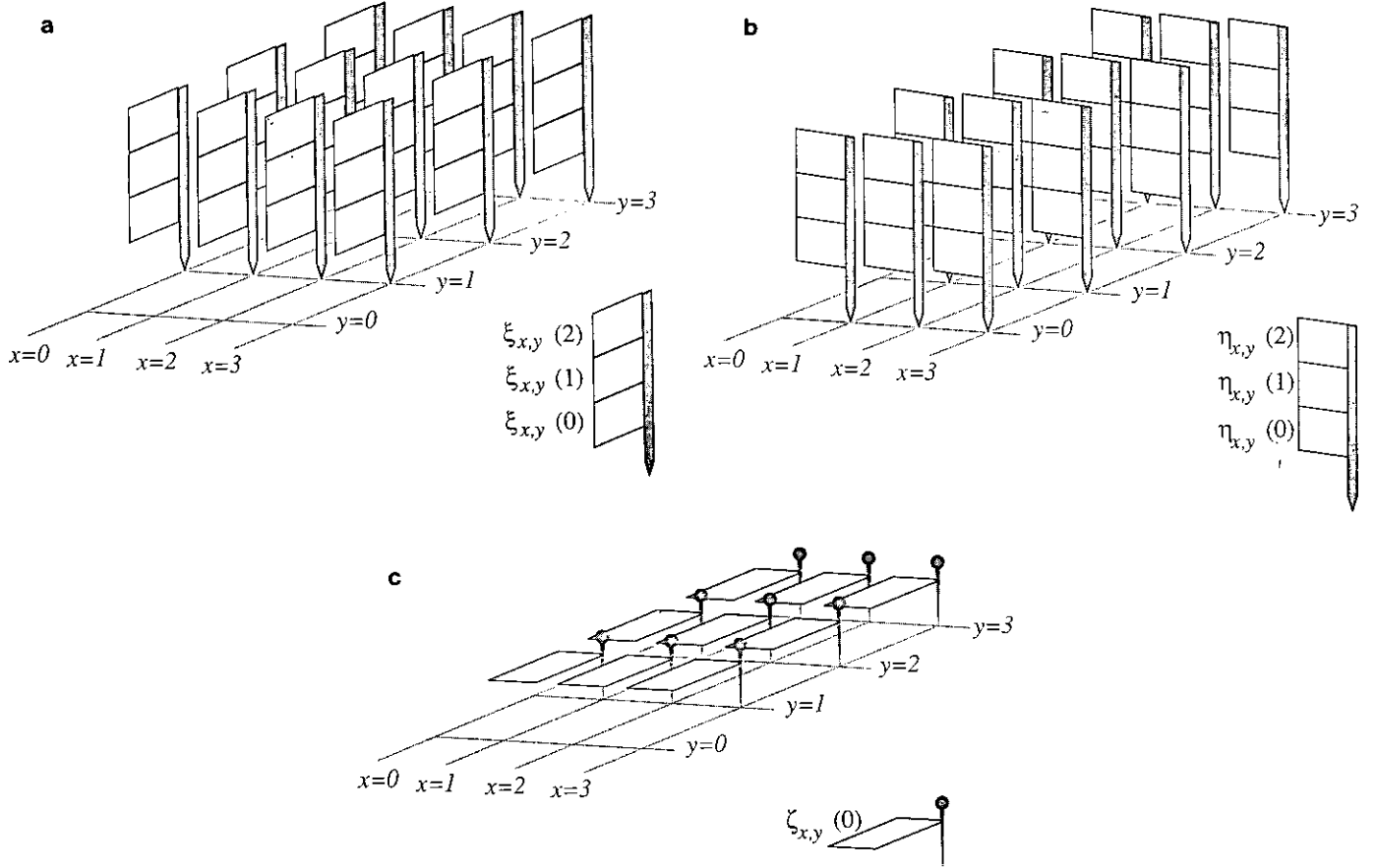


FIG. 5. Plaquette columns. Plaquettes (a) on  $yz$ -plane, (b) on  $zx$ -plane, and (c) on  $xy$ -plane. For each column, we assign an integer. For example,  $\xi_{x,y}$  is assigned to the column of plaquettes at  $(x, y)$  and  $\xi_{x,y}(k)$  represents  $(k+1)$ th bit of  $\xi_{x,y}$ .

loop  $L$  is represented by assembly of these integers  $\{\xi_{x,y}, \eta_{x,y}, \zeta_{x,y}\} \equiv i$ . The number of links in the  $x$ -direction in the closed loop  $L_i$  is given by

$$N_x(i) \equiv \sum_{1 \leq x \leq X, 0 \leq y \leq Y} \|\eta_{x,y} * (2\eta_{x,y}) * \zeta_{x,y} * \zeta_{x,y+1}\|, \quad (\text{B.1})$$

with

$$\zeta_{x,0} \equiv \zeta_{x,Y+1} \equiv 0.$$

The number of links in the  $y$ -direction is

$$N_y(i) \equiv \sum_{0 \leq x \leq X, 1 \leq y \leq Y} \|\xi_{x,y} * (2\xi_{x,y}) * \zeta_{x,y} * \zeta_{x+1,y}\|, \quad (\text{B.2})$$

with

$$\zeta_{0,y} \equiv \zeta_{X+1,y} \equiv 0,$$

and for the  $z$ -direction it is

$$N_z(i) \equiv \sum_{0 \leq x \leq X, 0 \leq y \leq Y} \|\xi_{x,y} * \xi_{x,y+1} * \eta_{x,y} * \eta_{x+1,y}\|, \quad (\text{B.3})$$

with

$$\xi_{x,Y+1} \equiv \eta_{X+1,y} \equiv 0.$$

Using Eqs. (B.1)–(B.3), we obtain the expression for the length of  $L_i$ ,

$$\|L_i\| \equiv N_x(i) + N_y(i) + N_z(i). \quad (\text{B.4})$$

### APPENDIX C: CALCULATION OF $\varphi(i)$

As shown in Section II,  $\varphi(i)$  is defined as the sum of all the contributions from plaquette configurations whose boundary is the closed loop  $L_i$ ,

$$\varphi(i) \equiv \sum_{\{S \text{ such that } \partial S = L_i\}} u^{|\partial S|}. \quad (\text{C.1})$$

Let us consider the "cube variable"  $\bar{\sigma}(c)$  that is the product of six plaquette variables around a cube  $c$ ,

$$\bar{\sigma}(c) \equiv \prod_{p \in \partial c} \sigma_p. \quad (\text{C.2})$$

If we recognize  $\sigma_p$  as a product of the link variables, then  $\bar{\sigma}(c) \equiv 1$ . That is,  $\bar{\sigma}(c)$  is an elementary closed surface. Let  $\mathbf{C}$  be the set of  $V_3$  cubes and  $C_i$  be a subset of  $\mathbf{C}$ :

$$\mathbf{C} \equiv \{c_0, c_1, \dots, c_{V_3-1}\}, \quad (\text{C.3})$$

$$C_i \subseteq \mathbf{C}, \quad 0 \leq i \leq 2^{V_3} - 1. \quad (\text{C.4})$$

Correspondence between a subset  $C$  and an integer  $i$  is defined as

$$a_n = \begin{cases} 1 & \text{if } c_n \in C, \\ 0 & \text{if } c_n \notin C, \end{cases} \quad (\text{C.5})$$

$$i \equiv \sum_n a_n 2^n.$$

Then  $C_i$  generates the  $i$ th closed surface,

$$\bar{\sigma}(C_i) \equiv \prod_{c \in C_i} \bar{\sigma}(c). \quad (\text{C.6})$$

Translation of cube configuration  $i$  to plaquette configuration  $m_i$  introduced in Appendix A is straightforward.

Now, calculate the function  $\varphi(i)$  for a given closed loop  $i \equiv \{\xi_{x,y}, \eta_{x,y}, \zeta_{x,y}\}$ , considered in Appendix B. Let us introduce Z-bit integers  $\omega_{x,y}$  ( $1 \leq x \leq X$ ,  $1 \leq y \leq Y$ ) (Fig. 6). Assembly of  $\{\omega_{x,y}\} \equiv \omega$  defines a cube configura-

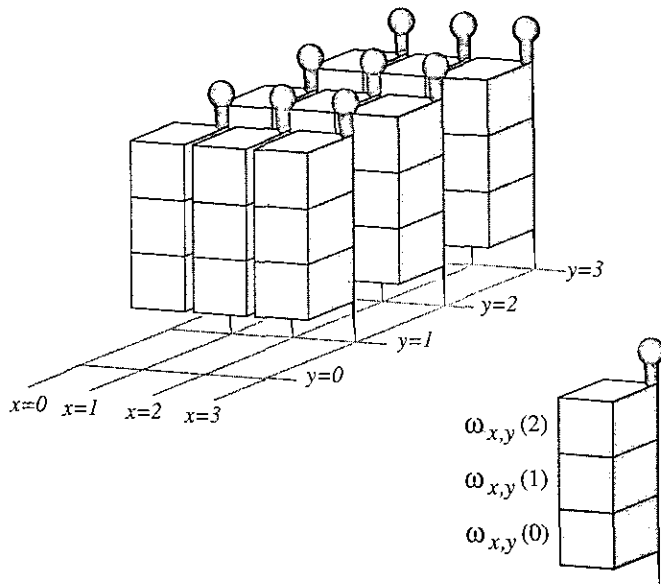


FIG. 6. Cube columns. Integer  $\omega_{x,y}$  is assigned to the column of cubes at  $(x, y)$ .  $\omega_{x,y}(k)$  represents  $(k+1)$ th bit of  $\omega_{x,y}$ .

tion or a closed surface. Fix the integers  $\omega$  and  $i$ . Then the number of the plaquette in the  $xy$  direction  $S_{xy}$  is

$$S_{xy}(\xi, \eta, \zeta, \omega) = \sum_{1 \leq x \leq X, 1 \leq y \leq Y} \|\zeta_{x,y} * \omega_{x,y} * (2\omega_{x,y})\|. \quad (\text{C.7})$$

Those in  $yz$  direction and  $xz$  are

$$S_{yz}(\xi, \eta, \zeta, \omega) = \sum_{0 \leq x \leq X, 1 \leq y \leq Y} \|\omega_{x,y} * \xi_{x,y} * \omega_{x+1,y}\|, \quad (\text{C.8})$$

with

$$\omega_{0,y} = \omega_{X+1,y} = 0 \quad (\text{C.9})$$

and

$$S_{xz}(\xi, \eta, \zeta, \omega) = \sum_{1 \leq x \leq X, 0 \leq y \leq Y} \|\omega_{x,y} * \eta_{x,y} * \omega_{x,y+1}\|, \quad (\text{C.10})$$

with

$$\omega_{x,0} = \omega_{x,Y+1} = 0. \quad (\text{C.11})$$

Adding all the contributions from  $\omega$ , we obtain the expression for  $\varphi$ ,

$$\varphi(\xi, \eta, \zeta) = \sum_{0 \leq \omega_{x,y} \leq 2^Z - 1} \mu^{(S_{xy} + S_{yz} + S_{xz})(\xi, \eta, \zeta, \omega)}. \quad (\text{C.12})$$

#### APPENDIX D: PROPERTIES OF THE FOURIER TRANSFORMATION

In this section, all integers are restricted to the  $M$ -bit integer,  $0 \leq \text{integer} \leq 2^M - 1$ . The Fourier transform matrix defined by Eq. (2.22) is

$$F_{i,j} \equiv (-1)^{\|i \cdot j\|}. \quad (\text{D.1})$$

The *self-inversion property* (Eq. (2.24)) is

$$\begin{aligned} (F^2)_{i,j} &= \sum_k (-1)^{\|i \cdot k\| + \|k \cdot j\|} \\ &= \sum_{0 \leq k \leq 2^M - 1} (-1)^{\|k \cdot (i+j)\|} \\ &= 2^M \delta_{i,j}. \end{aligned} \quad (\text{D.2})$$

Thus,

$$(F^{-1})_{i,j} \equiv \frac{1}{2^M} (-1)^{\|i \cdot j\|}. \quad (\text{D.3})$$



We diagonalize the potential term (Eqs. (2.25)–(2.26)):

$$\begin{aligned}\tilde{\varphi}_{i,j} &\equiv (F\varphi F^{-1})_{i,j} \\ &= \frac{1}{2^M} \sum_{k,l} (-1)^{\|i \cdot k\|} \varphi(k * l) (-1)^{\|l \cdot j\|}. \quad (\text{D.4})\end{aligned}$$

Let  $m \equiv k * l$ ; then  $l = k * m$ . Change the summation variables  $k, l$  to  $k, m$ ; then

$$\begin{aligned}\tilde{\varphi}_{i,j} &= \frac{1}{2^M} \sum_{k,m} (-1)^{\|i \cdot k\|} \varphi(m) (-1)^{\|(k * m) \cdot j\|} \\ &= \left( \frac{1}{2^M} \sum_k (-1)^{\|k \cdot (i * j)\|} \right) \left( \sum_m (-1)^{\|m \cdot j\|} \varphi(m) \right) \\ &= \delta_{i,j} \tilde{\varphi}_j, \quad (\text{D.5})\end{aligned}$$

where  $\tilde{\varphi}_i \equiv (F\varphi)_i$ .

The fast Fourier transformation (FFT) in this algorithm is exactly the same as the FFT algorithm in “ordinary Fourier transformation.” Fourier transformation  $\tilde{f}$  of  $f$  is defined as

$$\tilde{f}(p) \equiv \sum_x (-1)^{\|p \cdot x\|} f(x). \quad (\text{D.6})$$

Using a binary expression of  $x$  and  $p$ ,

$$\begin{aligned}x &\equiv x_0 2^0 + x_1 2^1 + \cdots + x_{M-1} 2^{M-1}, \\ p &\equiv p_0 2^0 + p_1 2^1 + \cdots + p_{M-1} 2^{M-1},\end{aligned} \quad (\text{D.7})$$

the Fourier transformation (D.6) is rewritten as bit-by-bit sums:

$$\begin{aligned}\tilde{f}(p_0, p_1, \dots, p_{M-1}) \\ &= \sum_{x_0} \sum_{x_1} \cdots \sum_{x_{M-1}=0,1} (-1)^{x_0 p_0} \\ &\quad \times (-1)^{x_1 p_1} \cdots (-1)^{x_{M-1} p_{M-1}} \\ &\quad \times f(x_0, x_1, \dots, x_{M-1}). \quad (\text{D.8})\end{aligned}$$

The above can be calculated by the recursion equation,

$$\begin{aligned}F_{k+1}(p_0, \dots, p_{k-1}, \underbrace{p_k}_{(k+1)\text{th bit}}, x_{k+1}, \dots, x_{M-1}) \\ &= \sum_{x_k=0,1} (-1)^{p_k x_k} \\ &\quad \times F_k(p_0, \dots, p_{k-1}, \underbrace{x_k}_{(k+1)\text{th bit}}, x_{k+1}, \dots, x_{M-1}), \quad (\text{D.9})\end{aligned}$$

with initial condition

$$F_0(x_0, x_1, \dots, x_{M-1}) \equiv f(x_0, x_1, \dots, x_{M-1}). \quad (\text{D.10})$$

Then the  $M$ th function is the Fourier transformed function

$$\tilde{f}(p_0, p_1, \dots, p_{M-1}) = F_M(p_0, p_1, \dots, p_{M-1}). \quad (\text{D.11})$$

The cost to perform the mapping is  $M 2^M$  steps.

## ACKNOWLEDGMENTS

The computer calculation has been done by using the computer centers of Yukawa Institute for Theoretical Physics, Kyoto University and the Institute for Nuclear Study, University of Tokyo. One of the authors (Y. S. H.) thanks Dr. K. Kasahara for useful discussions. This work was supported by the Kitasato Research Foundation under Grant H1-14.

## REFERENCES

1. C. N. Yang and T. D. Lee, *Phys. Rev.* **87**, 404 (1952); T. D. Lee and C. N. Yang, *ibid.* **87**, 410 (1952).
2. R. B. Pearson, *Phys. Rev. B* **26**, 6285 (1982).
3. H. Arisue and T. Fujiwara, *Progr. Theor. Phys.* **72**, 1176 (1984); *Nucl. Phys. B* **285** [FS19], 253 (1987).
4. K. Wilson, *Phys. Rev. D* **10**, 2445 (1974).
5. M. Creutz, L. Jacob, and C. Rebbi, *Phys. Rev. Lett.* **42**, 178 (1979).
6. Y. S. Hirata, *Progr. Theor. Phys.* **82**, 34 (1990).
7. K. Wilson, see J.-M. Drouffe and J.-B. Zuber, *Phys. Rep.* **102**, 1 (1983).